Supplementary Information

Tumor-derived ST3GAL1 promotes melanoma immune escape by stabilizing CD73 and activating the adenosine axis

Chiara De Vellis[1,2], Luisa Maresca[1,3], Silvia Pietrobono[1,4], Antonino Aparo[5], Adriana Maria Di Stefano[1,6], Francesco Massaini[3], Alessandro Giammona[1], Federica Ricci[1], Ilaria Battisti[7], Matteo Benelli[3], Giorgio Arrigoni[7], Barbara Stecca[1*]

This PDF file includes:

Supplementary Figures S1-S15

Supplementary Tables S1 to S2

Supplementary Figures

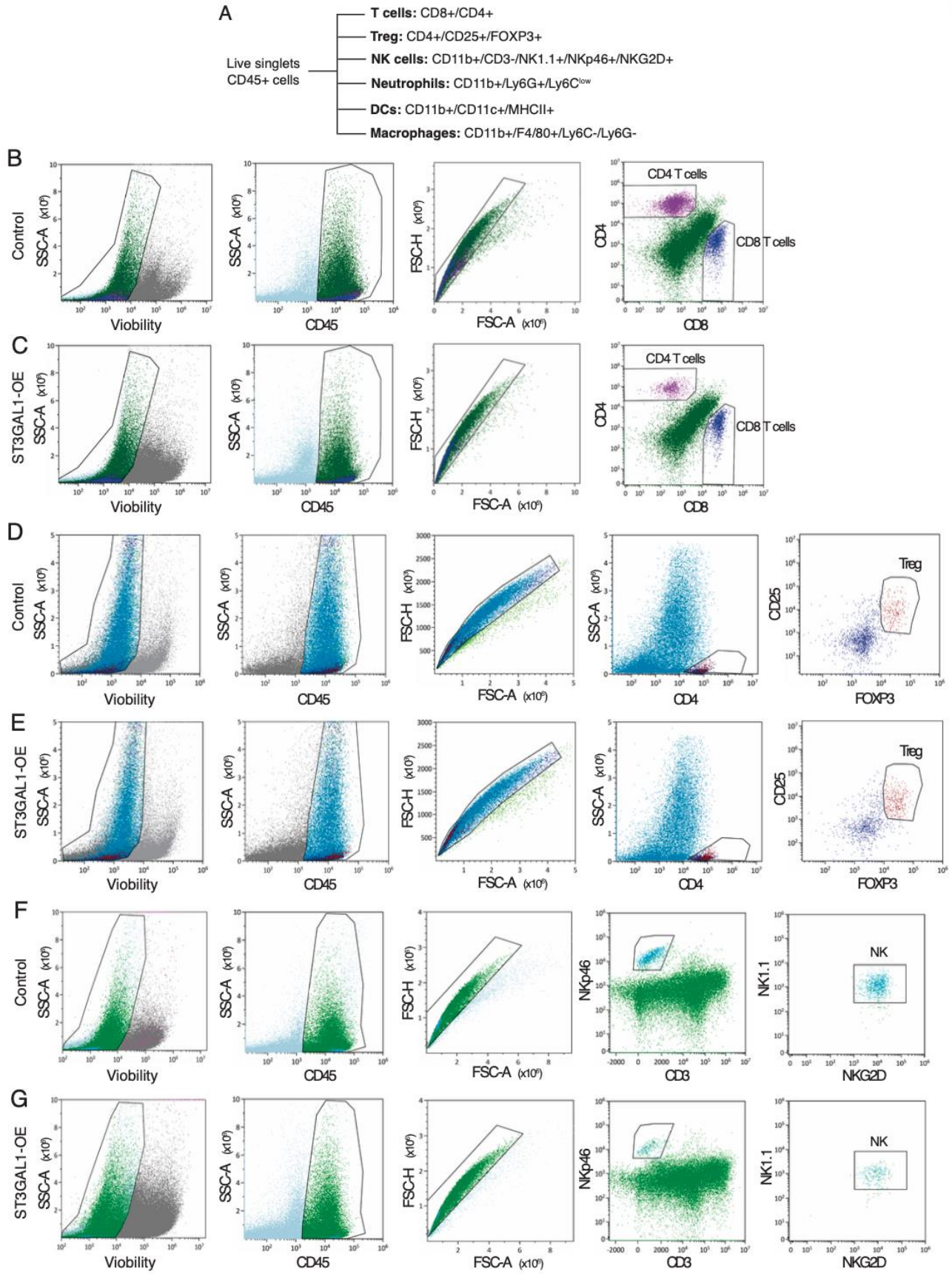

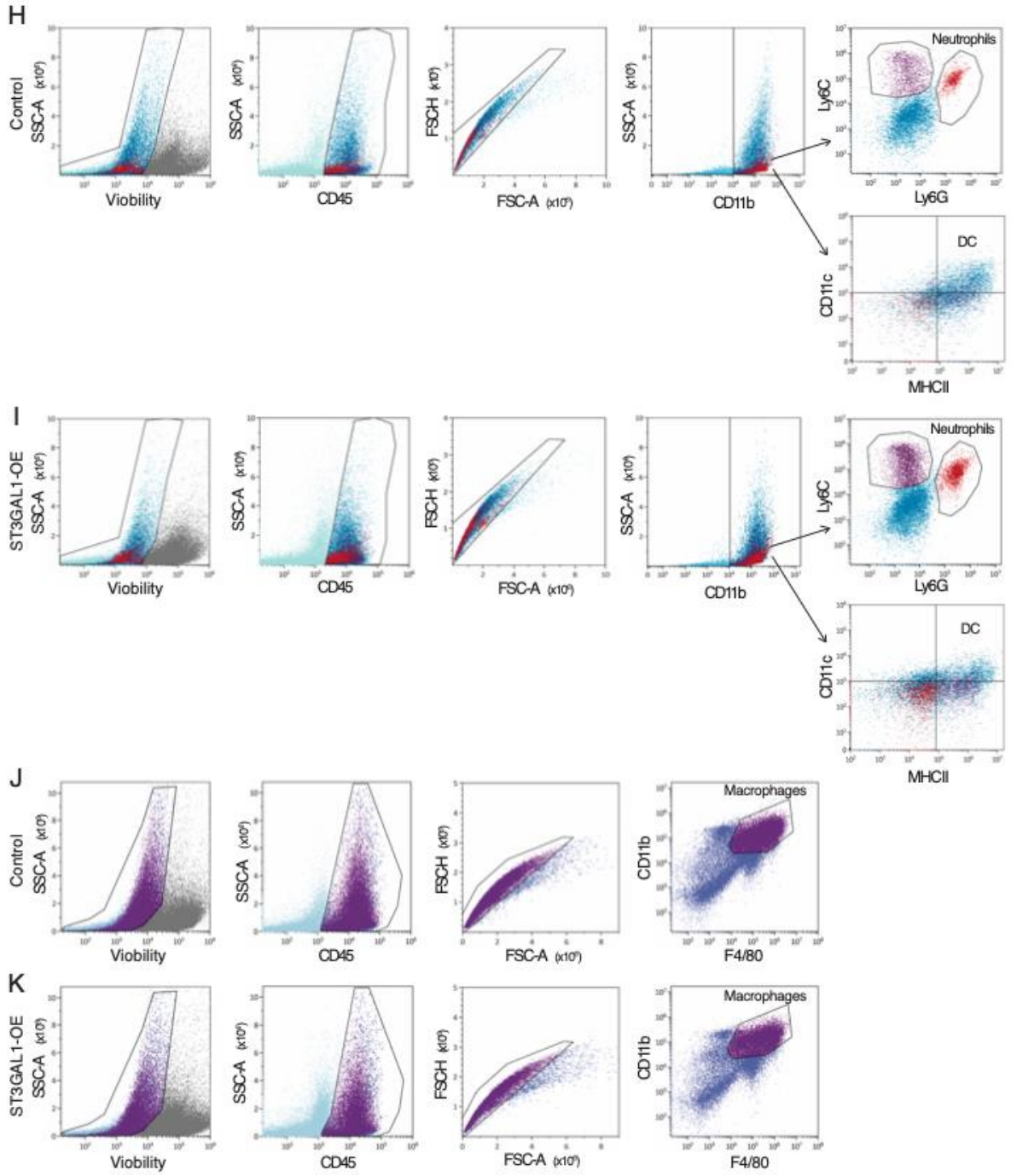

Fig. S1: Flow cytometry analysis and gating strategies for the identification of tumor infiltrating immune cells. (A) Schematic representation of markers used to identify tumor infiltrating immune populations. Following resection and single-cell dissociation of the tumor, viable immune cell populations were gated on CD45+ and doublets were excluded comparing FSC-H versus FSC-A. CD45+ immune cell infiltrates were identified based on the indicated markers. (**B-K)** Flow cytometry gating strategy used to determine the percentage of CD4+ and CD8+ T cells (**B,C**); Treg (**D,E**), natural killer (NK) cells (**F,G**), neutrophils and dendritic cells (DCs) (**H,I**), and macrophages (**J,K**) in control (pBABE) and ST3GAL1-OE B16F10 tumors. A representative tumor for each group is shown.

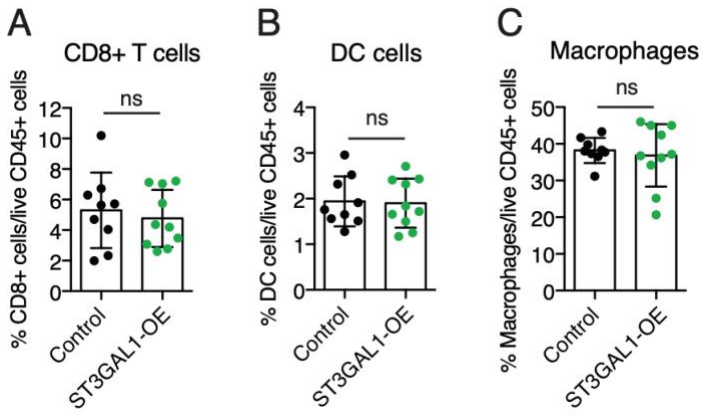

Fig. S2: Immune cell infiltration in ST3GAL1-OE allografts. Flow cytometry analysis of CD8+ T cells **(A)**, dendritic cells (DCs) **(B)**, and macrophages **(C)** in control (pBABE) (n=9) or ST3GAL1-OE (n=9) B16F10 tumors. Data represent mean ± SD. Unpaired Student *t* test; ns, not significant.

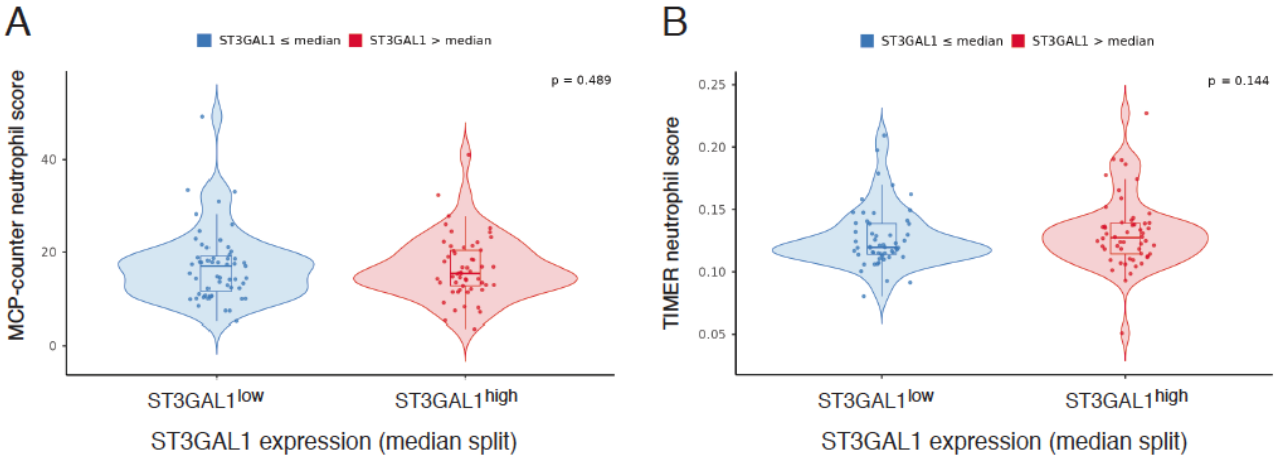

Fig. S3: Neutrophil infiltration in ST3GAL1^{low} and ST3GAL1^{high} metastatic melanomas. MCP-counter (p=0.489) **(A)** and TIMER (p=0.144) **(B)** neutrophil scores in ST3GAL1^{low} and ST3GAL1^{high} human metastatic melanomas (n=109).

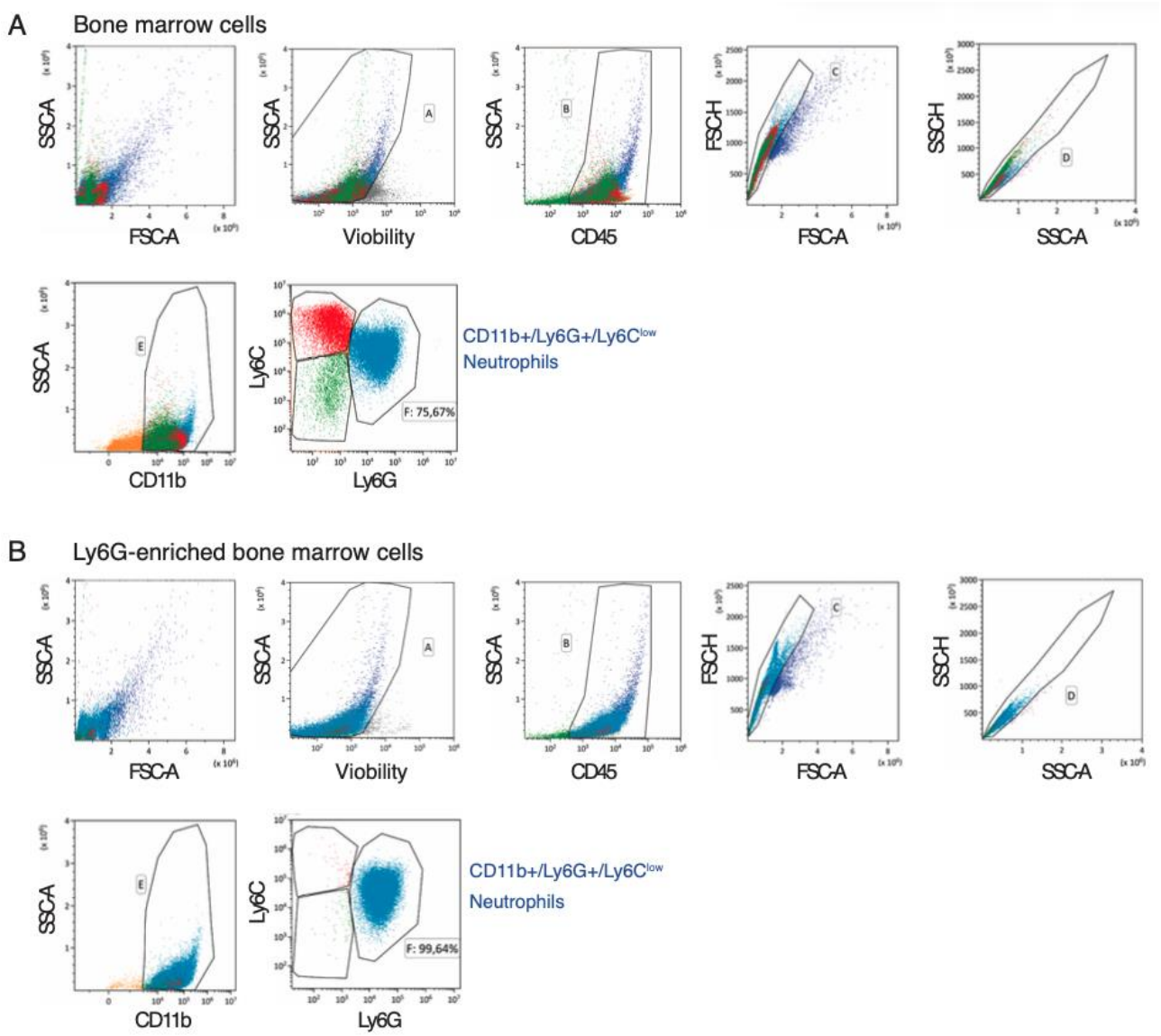

Fig. S4: Flow cytometry gating strategy used for the isolation of neutrophils from bone marrow cells. **(A)** Bone marrow cells. **(B)** Enrichment of Ly6G+ neutrophils from bone marrow cells of tumor-bearing mice. Ly6G+ cells were purified using anti-Ly6G microbeads. Cells were included on the total of captured events in SSC-A (side scatter) versus FSC-A (forward scatter) plot. Live cells (gate A) were discriminated from death cells using Viobility Fixable dye. CD11b+ cells were gated on CD45+ cells (gate B). Doublets were excluded as shown in gates C and D. CD11b+ cells were gated on CD45+ cells (gate E). Phenotype of CD45+/CD11b+ was determined by the expression of Ly6C and Ly6G markers. Neutrophils were CD45+/CD11b+/Ly6G+/Ly6C^{low}. Note that Ly6G+ bone marrow cell purification increases the proportion of neutrophils from 75% to 99%.

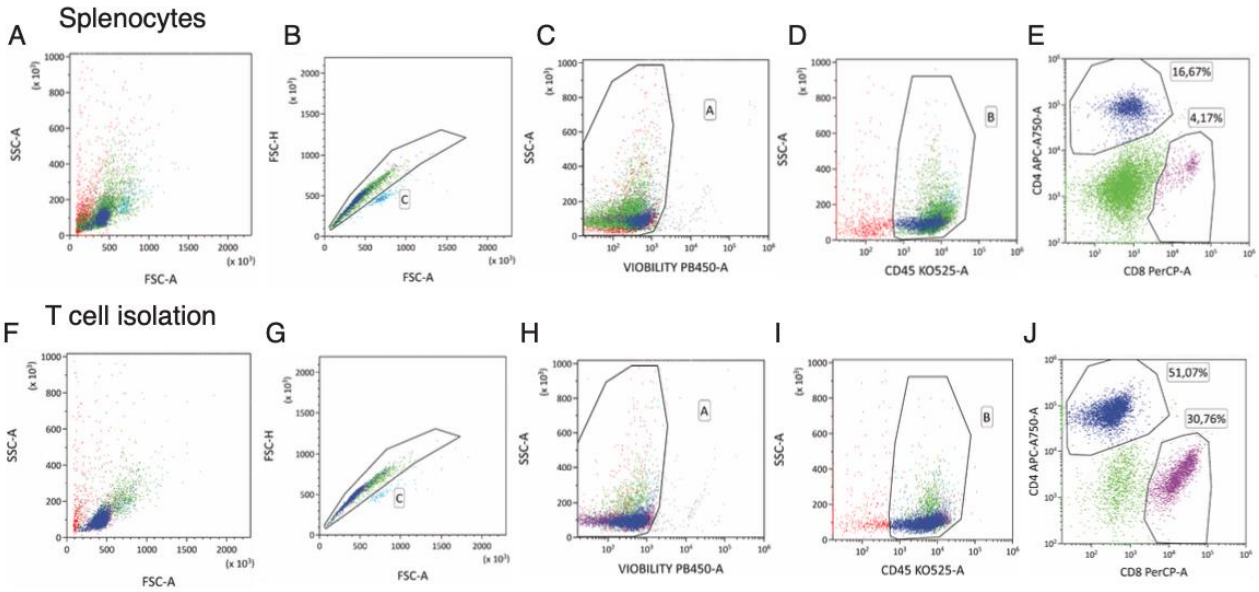

Fig. S5: Isolation of CD8+ and CD4+ T cells from spleen. Flow cytometry gating strategy used to determine the proportion of CD4+ and CD8+ T cells isolated from spleens (**A-E**) and after purification with mouse Pan T Cell Isolation Kit II (**F-J**). Doublets and dead cells were excluded as shown in gates C **(B,G)** and A **(C,H)**. CD4+ and CD8+ T cells **(E,J)** were gated on CD45+ cells **(D,I)**.

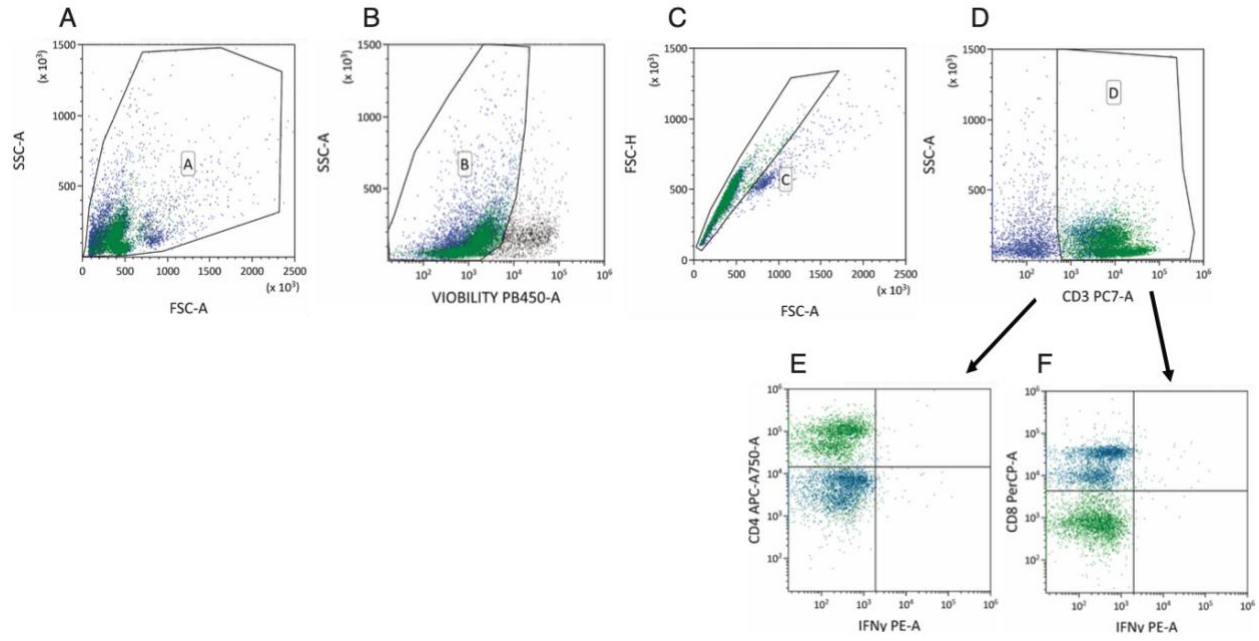

Fig. S6: Flow cytometry gating strategy of intracellular IFNγ. (A) Cells were included in Gate A on the total of captured events in SSC-A (side scatter) versus FSC-A (forward scatter). Dead cells and doublets were excluded as shown in (**B)** and (**C**). **(D-F)** The intracellular production of IFNγ in CD4+ (**E**) and CD8+ (**F**) T cells was evaluated on CD3+ cells (**D**).

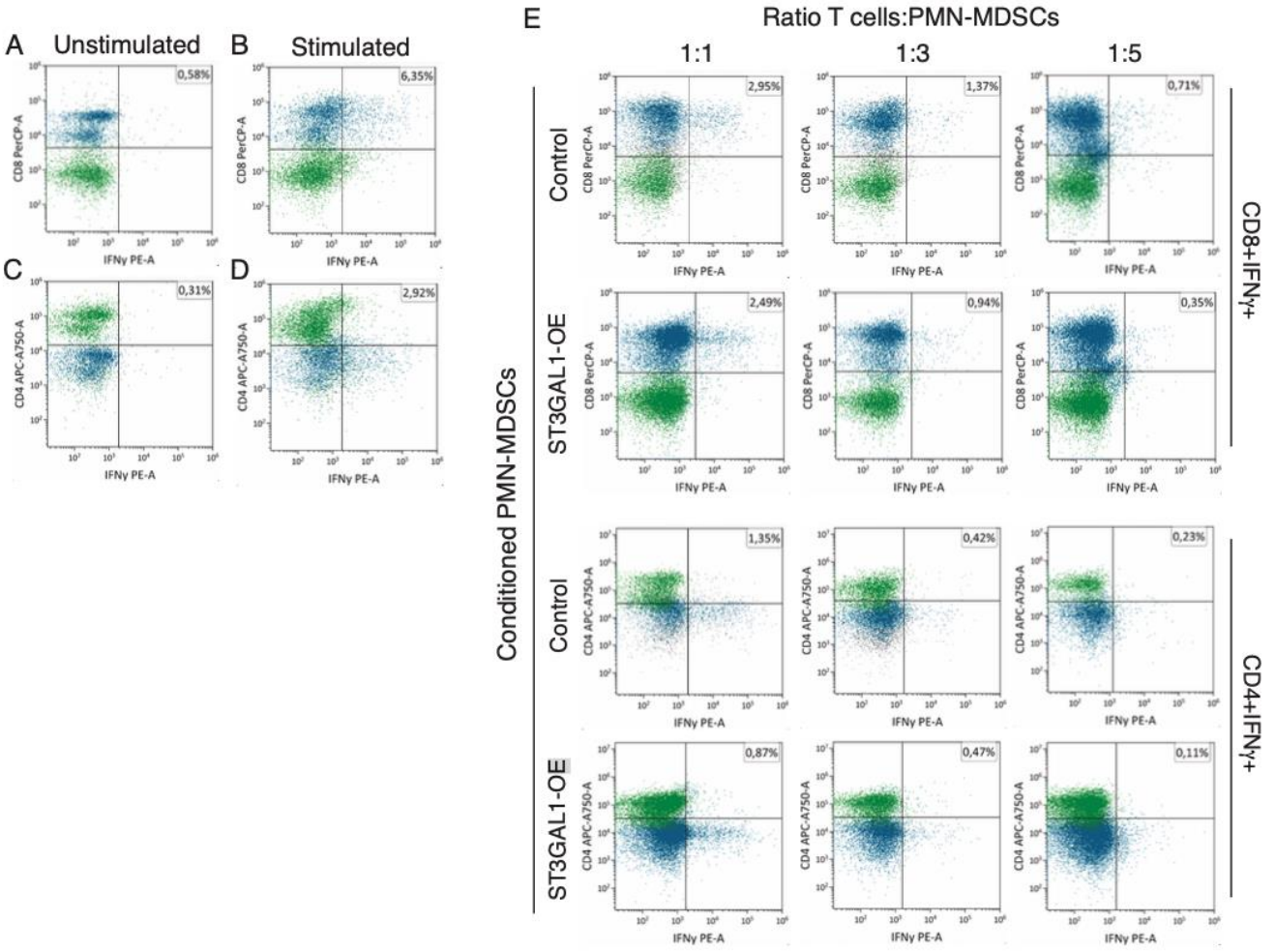

Fig. S7: Flow cytometry analysis of intracellular IFNγ. (A-D) Flow cytometry analysis of intracellular IFNγ in purified CD8+ and CD4+ T cells before **(A,C)** and after activation (**B,D**) with anti-CD3ε and anti-CD28. (**E**) Flow cytometry analysis of intracellular IFNγ in purified CD8+ and CD4+ T cells co-cultured for 48 hours with different ratios of PMN-MDSCs pre-conditioned for 48 hours with CM from Control or ST3GAL1-OE B16F10 cells.

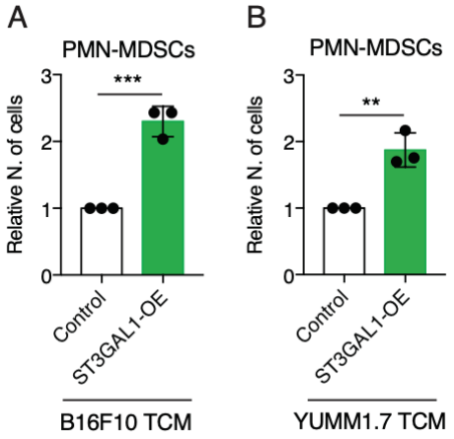

Fig. S8: Tumor conditioned media from ST3GAL1-OE melanoma cells sustain survival of PMN-MDSCs. Survival assay in PMN-MDSCs cultured 72 hours with TCM from B16F10 **(A)** or YUMM1.7 **(B)** cells transduced as indicated. Data represent mean ± SEM of at least three independent experiments. **p<0.01; ***p<0.001 (unpaired Student *t* test).

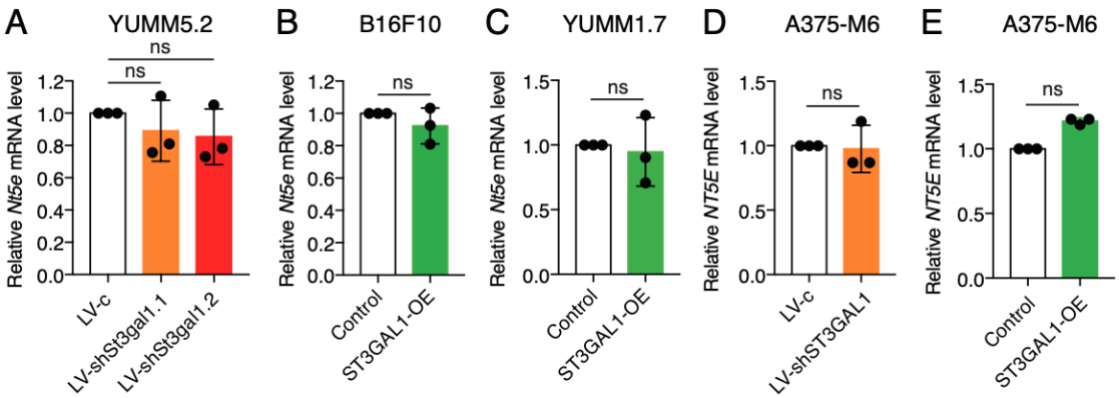

Fig. S9: Modulation of ST3GAL1 expression does not affect *NT5E* mRNA level in melanoma cells. qPCR of *Nt5e/NT5E* in murine **(A-C)** and human **(D,E)** melanoma cells transduced as indicated. Data represent mean ± SEM. One-way ANOVA (A); Unpaired Student's *t* test (B-E); ns, not significant.

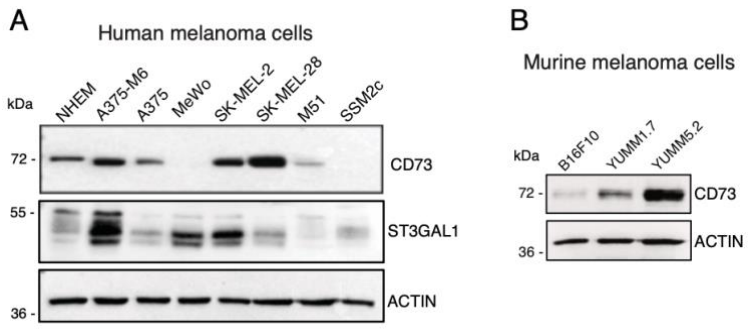

Fig. S10: CD73 and ST3GAL1 expression in human and murine melanoma cells. Western blot of CD73 and ST3GAL1 in normal human epidermal melanocytes (NHEM) and in a panel of human (**A**) and of CD73 in murine melanoma cell lines (**B**). ACTIN was used as loading control.

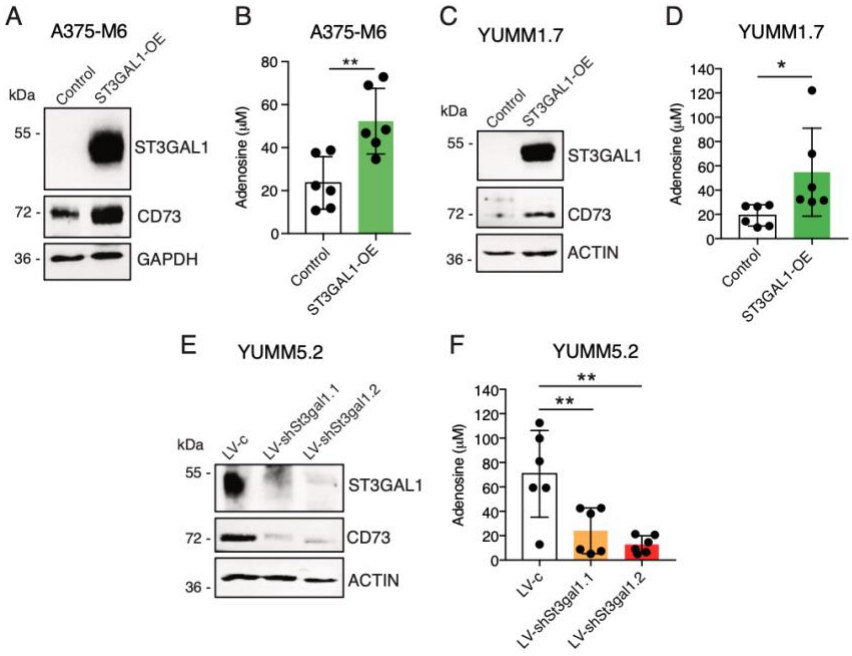

Fig. S11: Modulation of ST3GAL1 expression regulates extracellular adenosine production in melanoma cells. Western blot of ST3GAL1 and CD73 (**A,C**), and adenosine quantification (μM) (**B,D**) in the supernatants of A375-M6 (**A,B**) and YUMM1.7 (**C,D**) cells transduced with Control or ST3GAL1-OE. GAPDH or ACTIN were used as loading controls. Western blot of ST3GAL1 and CD73 (**E**), and adenosine quantification (μM) (**F**) in the supernatants of YUMM5.2 cells transduced with LV-c, LV-shSt3gal1.1 or LV-shSt3gal1.2. ACTIN was used as loading control. Data represent mean ± SD of at least three independent experiments. Significance was determined using unpaired Student *t* test (B,D); one-way ANOVA (E). *p<0.05; **p<0.01.

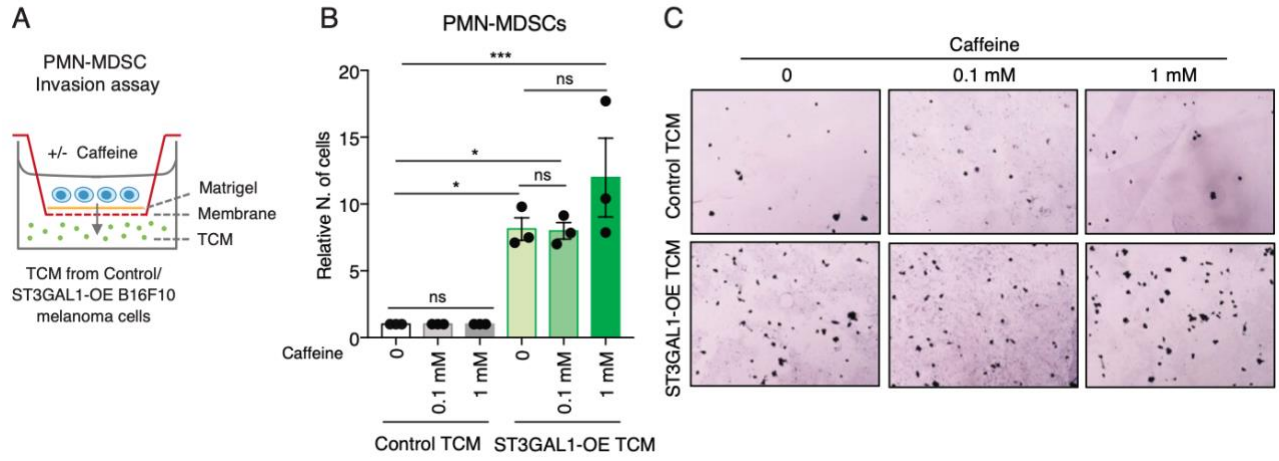

Fig. S12. Invasion assay of PMN-MDSCs upon caffeine treatment. (A) Schematic representation of PMN-MDSC invasion assay. PMN-MDSCs, cultured with vehicle (PBS) or increasing concentrations of caffeine, were seeded in the upper chamber of a Transwell precoated with Matrigel, and TCM from murine melanoma cells transduced with Control or ST3GAL1-OE were used as a chemoattractant in the lower chamber. The number of invading cells was counted after 48 hours. **(B)** Invasion assay of caffeine-treated PMN-MDSCs recruited by TCM from B16F10 cells transduced with Control or ST3GAL1-OE. Data represent mean ± SD of at least three independent experiments. Significance was determined using one-way ANOVA. *p<0.05; ***p<0.001; ns, not significant. **(C)** Representative pictures of (**B**).

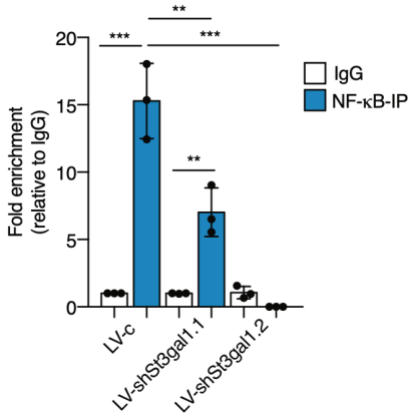

Fig. S13. ChIP-qPCR of NF-kB in YUMM5.2 cells. It shows that silencing of St3gal1 (LV-shSt3gal1.1 and LV-shSt3gal1.2) decreases NF-kB occupancy at *Ccl5* proximal promoter. The y-axis represents relative promoter enrichment, normalized on input material. IgG was set to 1. Data are expressed as mean ± SD. P value was calculated by one-way ANOVA with Tukey's correction (n=3). **, p<0.01; ***, p<0.001.

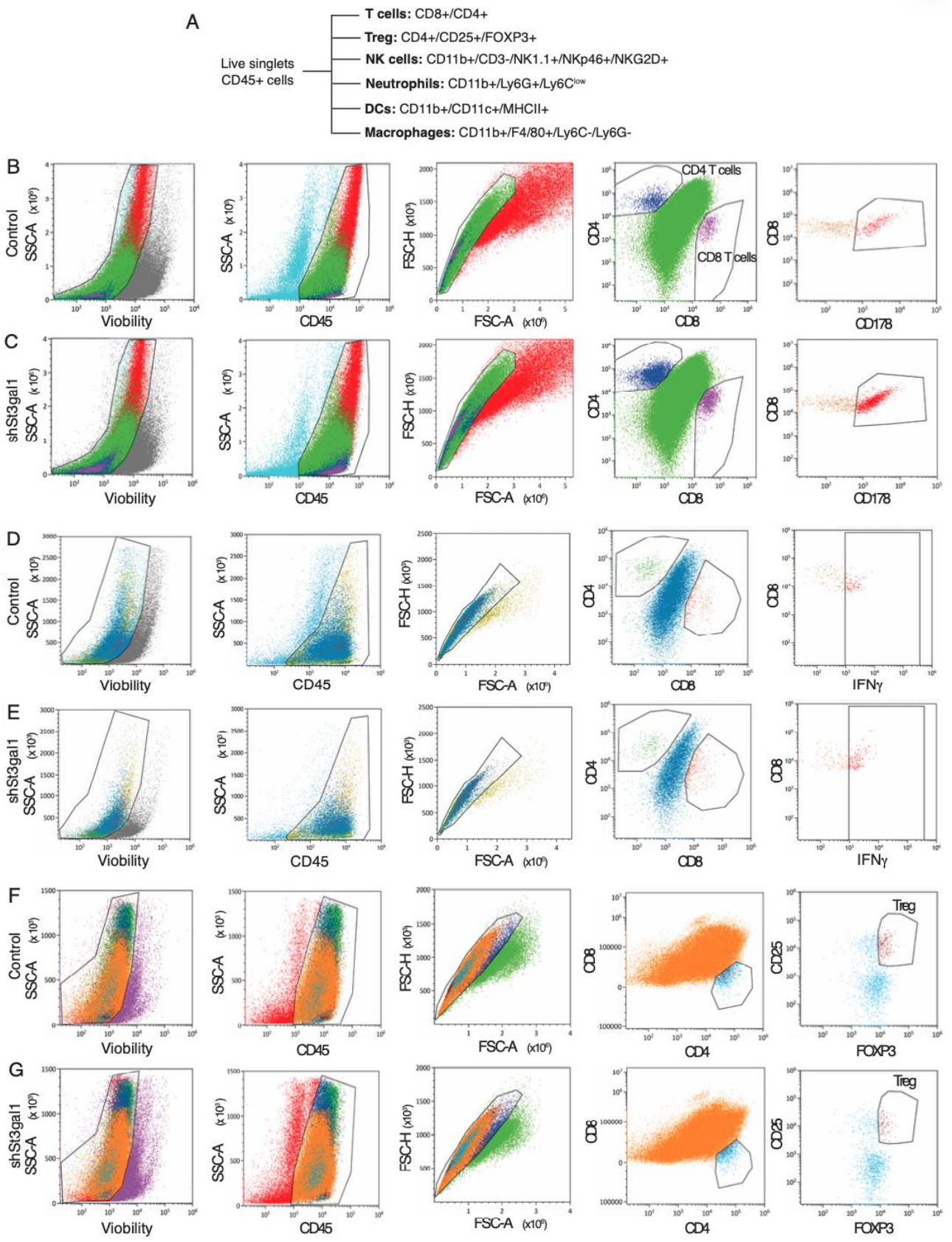
A
Live singlets
CD45+ cells
T cells: CD8+/CD4+
Treg: CD4+/CD25+/FOXP3+
NK cells: CD11b+/CD3-/NK1.1+/NKp46+/NKG2D+
Neutrophils: CD11b+/Ly6G+/Ly6C^low
DCs: CD11b+/CD11c+/MHCII+
Macrophages: CD11b+/F4/80+/Ly6C-/Ly6G-
B
C
D
E
F
G
Control
shSt3gal1
SSC-A
Viobility
CD45
FSC-H
FSC-A
CD4 T cells
CD8 T cells
CD4
CD8
CD178
IFNγ
Treg
CD25
FOXP3

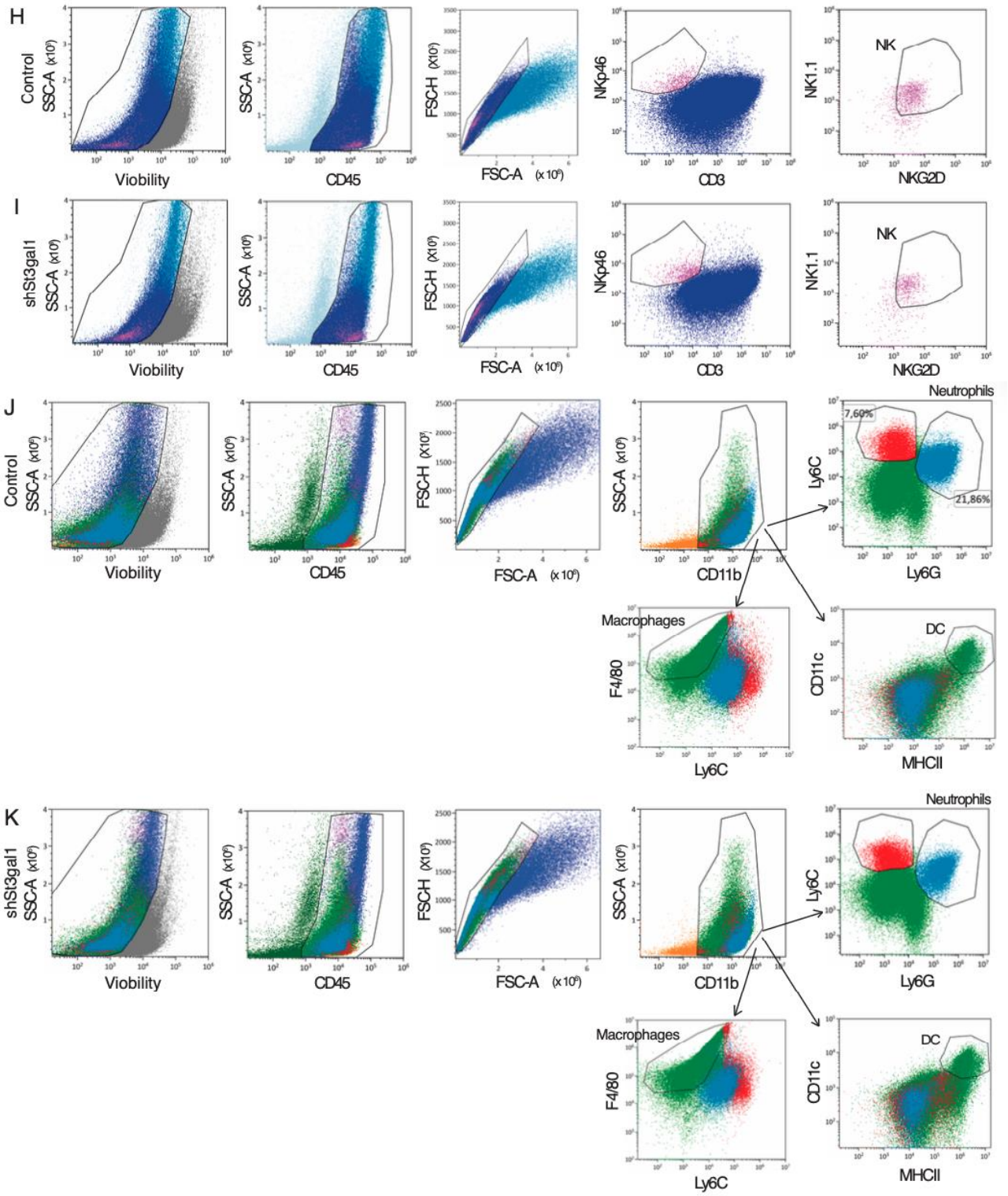

Fig. S14. Flow cytometry analysis and gating strategies used for the identification of tumor infiltrating immune cells. A) Schematic representation of markers used to identify tumor infiltrating immune populations. Following resection and single-cell dissociation of the tumor, viable immune cell populations were gated on CD45+ and doublets were excluded comparing FSC-H versus FSC-A. CD45+ immune cell infiltrates were identified based on the indicated markers. **B-K)** Flow cytometry gating strategy used to determine the percentage of CD4+ and CD8+ T cells, and CD8+CD178+ T cells (**B,C**); CD8+IFNγ+ T cells **(D,E)**; Treg (**F,G**), natural killer (NK) cells (**H,I**),

neutrophils, dendritic cells (DCs) and macrophages (**J**,**K**) in control (LV-c) and shSt3gal1 YUMM5.2 tumors. A representative tumor for each group is shown.

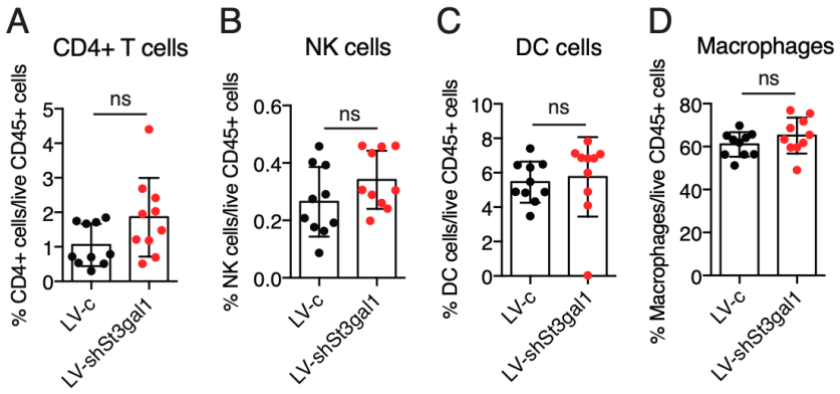

Fig. S15: Immune cell infiltration in *St3gal1*-silenced allografts. Flow cytometry analysis of CD4+ T cells **(A)**, natural killer (NK) **(B)**, dendritic cells (DCs) **(C)**, and macrophages **(D)** in control (LV-c) (n=10) or *shSt3gal1* (n=10) YUMM5.2 tumors. Data represent mean ± SD. Unpaired Student *t* test; ns, not significant.

Supplementary Tables

Table S1. List of primers used for qPCR.

Gene	Primer Sequence (5' to 3')
mCcl5	FW: GCTGCCCTCACCATCATCCT
	RV: CACTTGGCGGTTCCTTCGAG
mCcl5prom	FW: GTCTGGGCTACAACTTGGGA
	RV: GACTCTGCCTCTAACTGCCC
mNt5e	FW: TCCTGCAAGTGGGTGGAATC
	RV: CTCCACCGTTGGCCAGATAG
hNT5E	FW: CTCCTCTCAATCATGCCGCT
	RV: CAAATGTGCCTCCAAAGGGC
mGapdh	FW: TGACCACAGTCCATGCCATC
	RW: GACGGACACATTGGGGGTAG
mActin	FW: GGCTCCTAGCACCATGAAG
	RW: GAAAGGGTGTAAAACGCAGC
heIF2α	FW: GGATGGGACCTTGTTTGCCT
	RV: CCACGTTGCCAGGACAGTAT
hHPRT	FW: GCCAGACTTTGTTGGATTTG
	RV: CTCTCATCTTAGGCTTTGTATTTTG

Table S2. List of primary antibodies used for Western blotting.

Protein/Antibody	Origin	Catalog number	Company	Identifier
ST3GAL1 (WB)	Sheep	AF6905	R&D Systems	AB_3096968
ST3GAL1 (IP)	Mouse	MA564454	ThermoFisher Scientific	AB_3705541
CD73	Rabbit	13160	Cell Signaling Technology	AB_2716625
AXL	Mouse	sc-166269	Santa Cruz Biotechnology	AB_2243305
Integrin α5	Rabbit	#4705	Cell Signaling Technology	AB_2233962
pAKT (Ser473)	Rabbit	#9271	Cell Signaling Technology	AB_329825
AKT	Rabbit	sc-8312	Santa Cruz Biotechnology	AB_671714
pPKC (pan) (Thr514)	Rabbit	#9379	Cell Signaling Technology	AB_2252807
PKCα	Rabbit	#2056	Cell Signaling Technology	AB_2284227
pNF-kB (p65) (Ser536)	Rabbit	#3033	Cell Signaling Technology	AB_331284
NF-kB (p65)	Rabbit	#8242	Cell Signaling Technology	AB_10859369
CCL5/RANTES	Goat	AF478	R&D Systems	AB_355385
CCR5	Rat	MAB6138	R&D Systems	AB_10717978
PLCβ1	Rabbit	AB182359	Abcam	AB_2273656
iNOS	Rabbit	#13120	Cell Signaling Technology	AB_2687529
Vinculin	Mouse	sc-73614	Santa Cruz Biotechnology	AB_1131294
GAPDH	Mouse	sc-47724	Santa Cruz Biotechnology	AB_627678
ACTIN	Mouse	sc-47778	Santa Cruz Biotechnology	AB_626632